

Original Article

Exendin-4 protects kidney from acute ischemia-reperfusion injury through upregulation of NRF2 signaling

Yen-Yi Zhen^{1,3*}, Chih-Chao Yang^{2*}, Chi-Chih Hung¹, Chia-Chang Lee^{3,7}, Chen-Chang Lee⁷, Chien-Hsing Wu², Yen-Ta Chen⁴, Wei-Yu Chen³, Kuan-Hung Chen⁹, Hon-Kan Yip^{3,5,6,8,10#}, Sheung-Fat Ko^{7#}

¹Division of Nephrology, Department of Internal Medicine, Kaohsiung Medical University Hospital, Kaohsiung Medical University, Kaohsiung, Taiwan; ²Division of Nephrology, Department of Internal Medicine, ³Institute for Translational Research in Biomedical Sciences, ⁴Divisions of Urology, Department of Surgery, ⁵Center for Shockwave Medicine and Tissue Engineering, ⁶Division of Cardiology, Kaohsiung Chang Gung Memorial Hospital and Chang Gung University College of Medicine, Kaohsiung, Taiwan; ⁷Department of Radiology, Kaohsiung Chang Gung Memorial Hospital and Chang Gung University College of Medicine, Kaohsiung 833, Taiwan; ⁸Department of Medical Research, China Medical University Hospital, China Medical University, Taichung 40402, Taiwan; ⁹Department of Anesthesiology, Kaohsiung Chang Gung Memorial Hospital and Chang Gung University College of Medicine Kaohsiung 83301, Taiwan; ¹⁰Department of Nursing, Asia University, Taichung 41354, Taiwan, China. *Equal contributors. #Equal contributors.

Received August 5, 2017; Accepted October 16, 2017; Epub November 15, 2017; Published November 30, 2017

Abstract: This study tested the hypothesis that exendin-4 (Ex4) protects kidneys against ischemia-reperfusion (IR) injury mainly through upregulation of nuclear-factor erythroid 2-related factor 2 (Nrf2) signaling and downregulation of oxidative stress. Male-adult Sprague-Dawley rats (n=24) were equally divided into group 1 (sham-operated control), group 2 [IR only, ischemia (1 h)/reperfusion (72 h)] and group 3 (IR-Ex4, 10 µg/kg at 30 min, 24 h, 48 h after IR procedure). The in vitro study demonstrated that the protein expressions of phosphorylated (p)-Akt and Nrf2 were significantly progressively increased at time points of 0/0.5/1/3 h and 0/0.5/1/3/6/12/24 h, respectively in NRK-52E cells co-cultured with Ex4 (20 nM) (all P<0.0001). Additionally, the protein expressions of NOX-1/NOX2 were significantly increased, whereas p-Akt was significantly decreased in NRK-52E cells co-cultured with P-cresol (200 µM) that were significantly reversed after Ex4 treatment (all P<0.0001). As compared with baseline, the creatinine level, left/right kidney weight and MCP-1-positively stained area in the kidney parenchyma were significantly increased at 24 h after the IR procedure and significantly progressively decreased after that (all P<0.0001). By 27 h after IR, creatinine level/MCP-1 + area was significantly higher in group 2 than in groups 1 and 3, and significantly higher in group 3 than in group 1 (all P<0.0001). The numbers of Nrf2 +/NQO-1 + cells/SOD activity in kidney parenchyma were significantly lower in group 2 than in groups 1 and 3, and significantly lower in group 1 than in group 3 (all P<0.0001). In conclusion, Ex4 protected kidney from IR injury through upregulating antioxidants and downregulating inflammation/oxidative stress.

Keywords: Ischemia-reperfusion, kidney, anti-oxidant, oxidative stress, inflammation

Introduction

The kidney is a vital organ for clearance of toxic substances from the blood and maintains electrolyte/PH balance in the body [1-3]. On the other hand, the kidney and its vital functions are vulnerable to damage [i.e., resulting in acute kidney injury (AKI)] by many disease processes given its frequent exposure to reactive oxygen species (ROS)/oxidative stress and toxic organic/uremic substances and its sensitivity to hemodynamic instability such as after hypotensive shock [4-9]. In fact, AKI, which frequent-

ly occurs in hospitalized patients, includes a group of clinical syndromes that primarily manifest as a rapid decline in renal function in association with the accumulation of metabolic waste [10, 11]/uremic toxic substances such as p-Cresol, p-Cresyl sulfate and indoxyl sulfate [12, 13].

It is well recognized that acute ischemia-reperfusion (IR) injury of the kidney, in particular, is not only one of the most common factors to cause AKI, but it also constitutes a major health care problem with a high rate of in-hospital

Exendin-4 against IR renal injury through NRF2 signaling

mortality [14-17] and increased risk of long-term mortality [15, 18-21] despite current advances in medical treatment. This situation, therefore, warrants the development of new treatment modalities for improving kidney function after IR injury/AKI [8, 22, 23]. However, clarification of the underlying mechanism of acute kidney IR injury is pivotal for determining efficacious management for acute kidney IR injury.

Many studies have previously established that the underlying mechanism of acute organ IR injury, including acute kidney injury mainly involves a burst of reactive oxygen species (ROS)/oxidative stress from ischemic organ/tissue during reperfusion of ischemic tissues that can trigger the opening of the mitochondrial permeability transition pore, mitochondrial depolarization, decreased ATP synthesis and further increase the generation of ROS/oxidative stress [24-27]. These processes create a mediators, inflammatory cytokines, further oxidative stress and exacerbation of inflammation [24-27].

Exendin-4 (Ex4), a glucagon-like peptide-1 (GLP-1) analogue, was originally identified as a therapeutic agent for type 2 diabetes mellitus. Intriguingly, abundant data have demonstrated that Ex4 therapy has additional beneficial effects in the protection of tissues and organs from ischemic damage other than lowering the blood sugar [28, 29]. These effects are [2, 3] mainly through the anti-oxidative and anti-inflammatory properties of Ex4 [28-32]. Accordingly, this study, by utilizing in vitro and in vivo models of acute kidney IR injury tested whether Ex4 protected kidney against IR injury mainly through upregulation of nuclear-factor erythroid 2-related factor 2 (Nrf2) signaling and downregulation of the oxidative stress/inflammatory reaction.

Materials and methods

Ethics

All animal experimental protocols and procedures were approved by the Institute of Animal Care and Use Committee at Kaohsiung Chang Gung Memorial Hospital (Affidavit of Approval of Animal Use Protocol No. 2015091401) and performed in accordance with the Guide for the Care and Use of Laboratory Animals [The Eighth Edition of the Guide for the Care and Use of Laboratory Animals (NRC 2011)].

Animals were housed in an Association for Assessment and Accreditation of Laboratory

Animal Care International (AAALAC)-approved animal facility in our hospital (IACUC protocol no. 101008) with controlled temperature and light cycles (24°C and 12/12 light cycles).

Acute kidney ischemia-reperfusion protocol

The acute kidney ischemia-reperfusion (IR) was performed according to a previously published protocol [33]. Briefly, animals were anesthetized with 2% isoflurane and placed supine on a warming pad at 37°C for midline laparotomies. The sham control (SC) animals underwent laparotomy only. Acute IR injury of both kidneys was induced by clamping the renal pedicles of the rats with non-traumatic vascular clips for 60 minutes (i.e., ischemia was settled for 1 h) followed by reperfusion time points at 6 h, 24 h, 72 h and 168 h for blood sampling (i.e., a blood sample was drawn at these time intervals for examining the creatinine level). The animals were then euthanized by day 7 after IR procedure and the kidneys were harvested for further experiments.

Animal grouping

The rats were categorized into three groups (n=8 group): (1) group 1 (sham control), group 2 (IR) and group 3 [IR + Ex4 (10 µg/kg at 30 min, 24 h, 48 h after IR procedure)]. The dosage of Ex4 was based on our previous reports [28, 29, 31-33].

Renal histochemical analysis

Kidneys were fixed in an aqueous formaldehyde solution (37% w/w) containing sodium phosphates to provide buffering to an approximately isotonic solution with pH 7.2-7.6. After formaldehyde fixation, the kidneys were processed and embedded in paraffin. The paraffin kidney tissue block was cut into slices 4 µm thick with a RM2255 microtome (Leica Microsystems GmbH, Wetzlar, Germany). The paraffin sections were stained with haematoxylin and eosin (H&E) or Masson's trichrome. Additionally, the paraffin kidney tissue block was sliced at 4 µm and immunohistochemically stained with the following antibody: monocyte chemoattractant protein-1 (MCP-1) (Cell Signaling). The specimens were treated with commercially available peroxidase IHC kits (Thermo Scientific Pierce, Rockford, USA) and developed with dimainobenzidine (DAB) in staining buffer (Thermo Scientific Pierce). After staining, the slides were scanned with a Panoramic MIDI digital scanner

Exendin-4 against IR renal injury through NRF2 signaling

(3DHISTECH, Budapest, Hungary). Selection of the desired areas and adjustments were performed with the Panoramic Viewer 1.15 (3DHISTECH, Budapest, Hungary). Brightness and contrast were adjusted by using Photoshop CS4 (Adobe Systems, San Jose, USA).

Cell culture and treatment

In our *in vitro* study, the NRK-52E cells (a commercialized rat renal proximal tubular cell line from Sigma) were grown in Dulbecco's modified Eagle's medium with 4.5 g of glucose/l (DMEM) supplemented with 4% (w/v) glutamine, 100 µg/mL penicillium/streptomycin and 10% (v/v) fetal bovine serum, designated as normal DMEM, in a 100 µm polystyrene petri dish in an atmosphere of 5% CO₂/95% air at 37°C. For p-Cresol administration, the cells were seeded on a 100 µm petri dish and grown in normal DMEM for 24 hours, and then the cells were grown in p-cresol containing DMEM for another 24 hours. For exendin-4 stimulation, the cells were seeded in normal DMEM for 24 hours, and then 20 nM exendin-4 was added to stimulate cells for various durations.

Immunoblot

Cells were trypsinized and 10⁷ cells were resuspended in 1 ml hypotonic buffers (10 mM HEPES pH 7.9, 1.5 mM MgCl₂, 10 mM KCl, 0.5 mM DTT, protein inhibitor, phosphatase inhibitor) for 1 h. The cells were then homogenized with Dounce homogenizer with 120 strokes. The cell lysate was centrifuged at 250 x g at 4°C for 5 minutes. The cytoplasmic fraction was collected as the supernatant and the pellet, as the nuclear fraction, was resuspended in 1 ml Ripa buffer (Sigma).

Protein concentration was determined using Bradford protein assay kit (BioRad). Then 30 µg of proteins from the total cell lysate, nuclear fraction, or cytoplasmic fraction were resolved on 8 or 10% SDS-poly-acrylamide gel. After protein migration, the proteins were blotted on PVDF membrane (Immobilon 0.45 m, Millipore). The membranes were blocked in 5% silk milk for 2 h in TBST buffer (20 mM Tris-Cl, 150 mM NaCl, 0.1% Tween 20, pH 7.4). After blocking, membranes were incubated with first antibodies [total Akt (1:1000, Cell Signaling), phosphorylated (p)-Akt (1:1000, Cell Signaling), NOX-1 (1:1500, Sigma), NOX-2 (1:750, Sigma), Nrf2 (1:200; Santa Cruz Biotechnology) and NQO1

(1:200; Santa Cruz Biotechnology) for 2 h. Subsequently, the membranes were incubated with the desired secondary antibody for another 2 h. Immuno-reactive signals were detected by incubation with horseradish peroxidase conjugated-secondary followed by enhanced chemiluminescent detection using Pierce ECL Western Blotting Substrate (Thermo Scientific). Immunoblot imaging was captured by using a BioSpectrum AC Imaging System (Ultra-Violet Products). The protein bands were quantified using ImageQuant software (GE-Healthcare) and digitally converted for statistical analysis.

Immunofluorescence staining and immunofluorescence microscopy findings

An Olympus BX-51 epifluorescence microscope (Olympus, Kyoto, Japan) equipped with X-Cite XCT10A (Lumen Dynamics, Wiesbaden, Germany) light source, filters and 10x, 20x, 40x, 60x, and 100x was used to observe the cells. The cells were seeded on 12 mm coverslip in a 24-well culture plate. Cells were harvested and fixed in 4% paraformaldehyde in CSK buffer (10 mM Pipes, 100 mM NaCl, 3 mM MgCl₂, 1 mM EGTA, 300 mM sucrose, pH 6.8) for 10 minutes, and permeabilized in 0.5 % Triton in CSK buffer for 5 minutes. After fixation, the cells were subjected to antibody staining. The antibodies used were as follows: NQO1 (1:500, Santa Cruz Biotechnology) and Nrf2 (1:300, Cell Signaling). Additional reagents used were TRITC/FITC phalloidin (1:1000; Sigma-Aldrich), and DAPI (1:500, Sigma-Aldrich). Cell nuclei were stained with 0.2 µg/mL 4',6-diamidino-2-phenylindole (DAPI; Sigma).

Superoxide dismutase assay and determination of serum creatinine concentration

Kidney tissue (0.2 g) was minced and homogenized in lysis buffer (0.5% Triton X-100, 5 mM β-mercaptoethanol, 0.1 mg/mL PMSF) for superoxide dismutase (SOD) assay. Additionally, serum creatinine level was determined using a modified Jaffe's reaction.

Statistical analysis

Quantitative data are expressed as means ± SD. Statistical analysis was adequately performed by ANOVA followed by Bonferroni multiple-comparison post hoc test. Statistical analysis was performed using SAS statistical software for Windows version 8.2 (SAS institute,

Extendin-4 against IR renal injury through NRF2 signaling

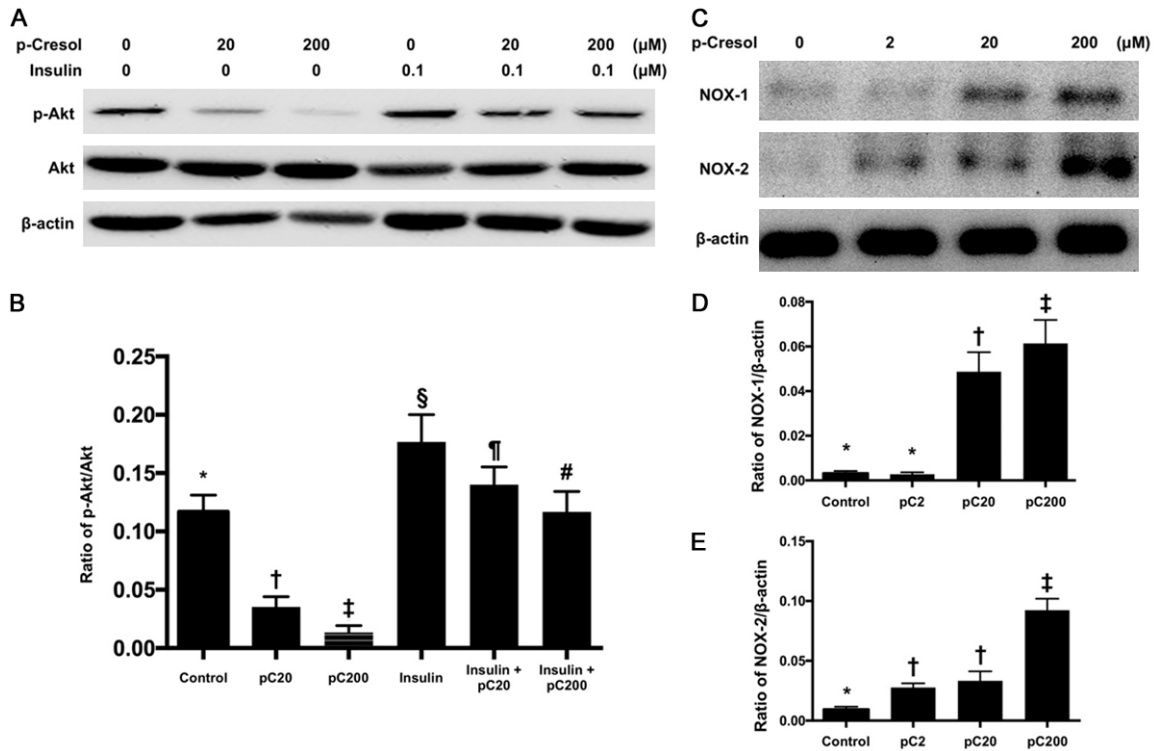


Figure 1. P-cresol enhanced oxidative stress and suppressed the phosphorylation of Akt in culturing NRK-52E cells. A. Illustrating the protein expressions of total Akt and phosphorylated (p)-Akt undergoing the stepwise-increased p-cresol (0, 20, 200 μM) treatment with and without insulin in the culture medium (0.1 μM). B. Analytical result of ratio of p-Akt/Akt, * vs. other groups with different symbols (†, ‡, §, ¶, #), $p < 0.0001$. C. Illustrating the protein expressions NOX-1 and NOX-2 undergoing the stepwise-increased p-cresol (0, 2, 20, 200 μM) treatment. D. Analytical result of protein expression of NOX-1, * vs. other groups with different symbols (†, ‡), $p < 0.0001$. E. Analytical result of protein expression of NOX-2, * vs. other groups with different symbols (†, ‡), $p < 0.0001$. All statistical analyses were performed by one-way ANOVA, followed by Bonferroni multiple comparison post hoc test ($n = 6$ for each group). Symbols (*, †, ‡, §, ¶, #) indicate significance at the 0.05 level. PC = p-cresol.

Cary, NC). A probability value of less than 0.05 was considered statistically significant.

Results

p-Cresol enhanced oxidative stress and suppressed the phosphorylation of Akt (Figure 1)

To elucidate the impact of P-cresol (i.e., a uremic toxic substance) on augmenting the oxidative stress and suppressing the phosphorylation (p) of Akt, in vitro study was conducted by using NRK-52E cells. The Western blot result showed that the ratio of p-Akt/Akt was significantly progressively suppressed by a stepwise increase in P-cresol (i.e., from 0, 20, 200 μM). However, this ratio was significantly reversed after administration of insulin in the culture medium (0.1 μM) (i.e., insulin can upregulate serine/threonine protein kinase Akt/PI3K), suggesting that P-cresol is harmful for cell survival, growth and proliferation.

As expected, the protein expressions of NADPH oxidase (NOX)-1 and NOX-2, two indicators of oxidative stress, were also significantly progressively enhanced by a stepwise increase of P-cresol (i.e., from 0, 2, 20, 200 μM).

Ex4 treatment upregulated the protein expressions of p-Akt and Nrf2 in NRK-52E cells (Figure 2)

Under Ex4 (20 nM) stimulation, the protein expression of p-Akt in NRK-52E cells was significantly progressively increased at four time points of 0, 0.5, 1 and 3 h, followed by significantly decreased at time intervals of 6, 12 and 24 h. On the other hand, the protein expression of Nrf2 was significantly progressively increased across these 7 time intervals.

To determine whether Ex4 independently-Akt regulated Nrf2 to attenuate oxidative stress, the compound LY294002, a strong inhibitor of

Exendin-4 against IR renal injury through NRF2 signaling

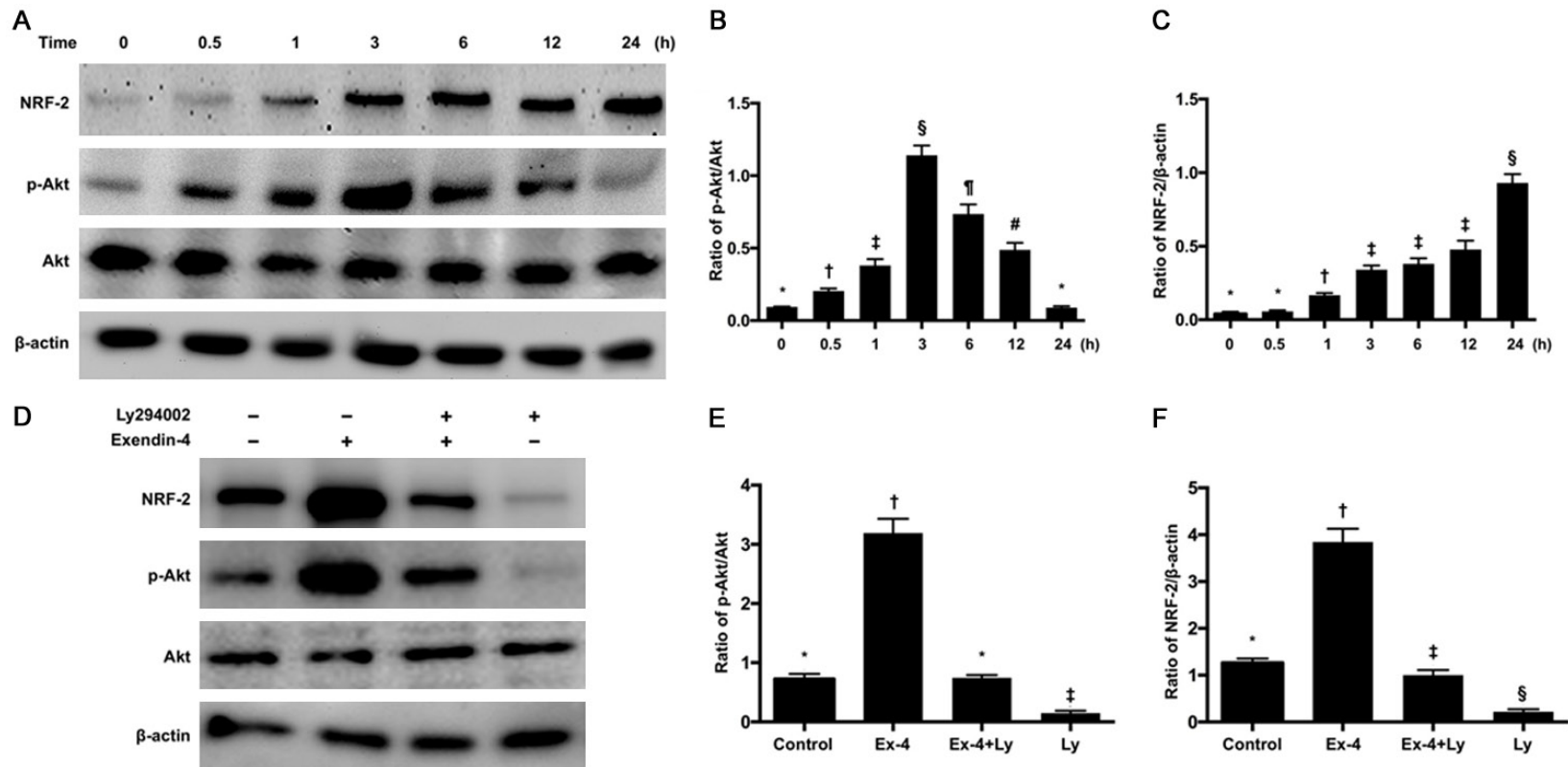


Figure 2. Exendin4 (Ex4) treatment upregulated the protein expressions of p-Akt and Nrf2 in NRK-52E cells. A. Illustrating the time courses of protein expressions of phosphorylated (p)-Akt and Nrf2 undergoing the Ex (20 nM) stimulation. B. Analytical result of ratio of p-Akt/Akt, * vs. other groups with different symbols (†, ‡, §, ¶, #), $p < 0.0001$. C. Analytical result of protein expression of Nrf2, * vs. other groups with different symbols (†, ‡, §), $p < 0.0001$. D. Illustrating the protein expressions of p-Akt and Nrf2 in NRK-52E cells in the present and absent conditions of LY294002 and Ex4 treatment, respectively. E. Analytical result of ratio of p-Akt/Akt protein expression, * vs. other groups with different symbols (†, ‡), $p < 0.0001$. F. Analytical result of protein expression of Nrf2, * vs. other groups with different symbols (†, ‡, §), $p < 0.0001$. All statistical analyses were performed by one-way ANOVA, followed by Bonferroni multiple comparison post hoc test ($n=6$ for each group). Symbols (*, †, ‡, §, ¶, #) indicate significance at the 0.05 level.

Extendin-4 against IR renal injury through NRF2 signaling

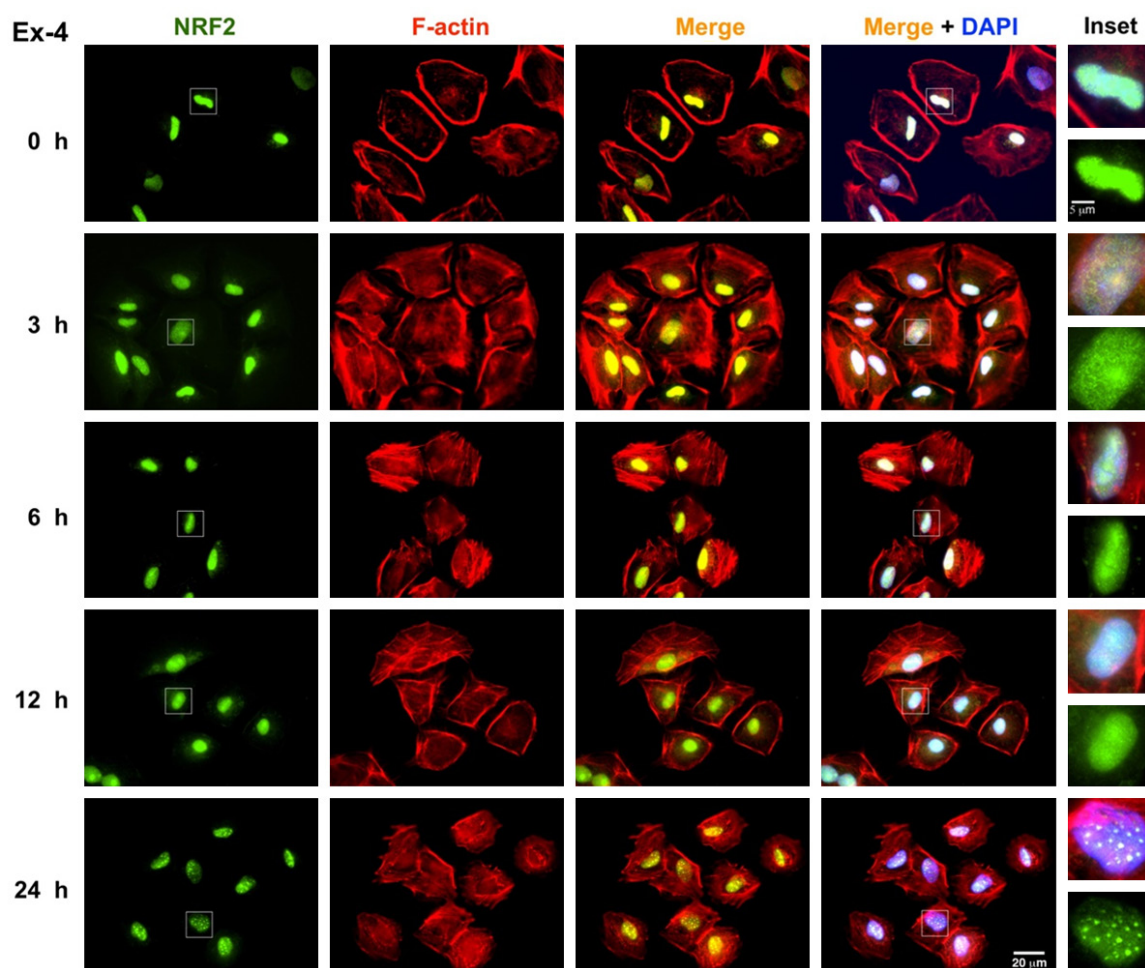


Figure 3. Immunofluorescent (IF) microscopic finding of NRF2 expression of in NRK-52E cells. The IF microscopic finding (400x) illustrated the time courses of TNrf2 in the NRK-52E cells undergoing the Ex4 stimulation for various time points (i.e., 0, 3, 6, 12 and 24 h). As noted in IF imaging (1000x), the Nrf2 appeared punctate in the nuclei of NRK-52E cells after 3 h Ex4 stimulation, and expressed as nuclear-body like pattern at 24 hours after Ex4 stimulation (refer to right column, i.e., inset). Ex-4 = extendin 4, p-Akt = phosphorylated Akt.

phosphoinositide 3-kinases (PI3Ks), was utilized for co-culture with NRK-52E (i.e., in the presence and absence of Ex4 treatment, respectively) to inhibit the expression of Nrf2 and the phosphorylation of Akt [i.e., to test the specificity of LY294002 for blocking the Akt/protein kinase B (PKB) signaling pathway]. As expected, the protein expression of Nrf2 and p-Akt was significantly increased after Ex4 treatment that was significantly suppressed after LY294002 treatment, suggesting that Ex4 independently-Akt activated Nrf2 signaling.

Ex4 stimulated the expression of NRF2 in NRK-52E cells (Figure 3)

To elucidate the expression of Nrf2 in the NRK-52E cells, the NRK-52E cells were incubated in

medium supplemented with Ex4 for various durations. As noted in immunofluorescence imaging, the Nrf2 appeared punctate in the nuclei of NRK-52E cells after Ex4 stimulation for 3 h, and was expressed as a nuclear-body like pattern at 24 h after Ex4 stimulation, demonstrating that Ex4 treatment upregulated the generation/distribution of Nrf2 in nuclei of NRK-52E cells.

Competitive effects of P-cresol vs. Ex4 in protein expression of antioxidants and oxidative stress in NRK-52E cells undergoing 24 h cell culture (Figure 4)

The protein expression of NOX-1 and NOX-2 in NRK-52E cells, two indicators of oxidative stress, were significantly upregulated by stimulation with P-cresol (200 µM) for 24 h. However,

Extendin-4 against IR renal injury through NRF2 signaling

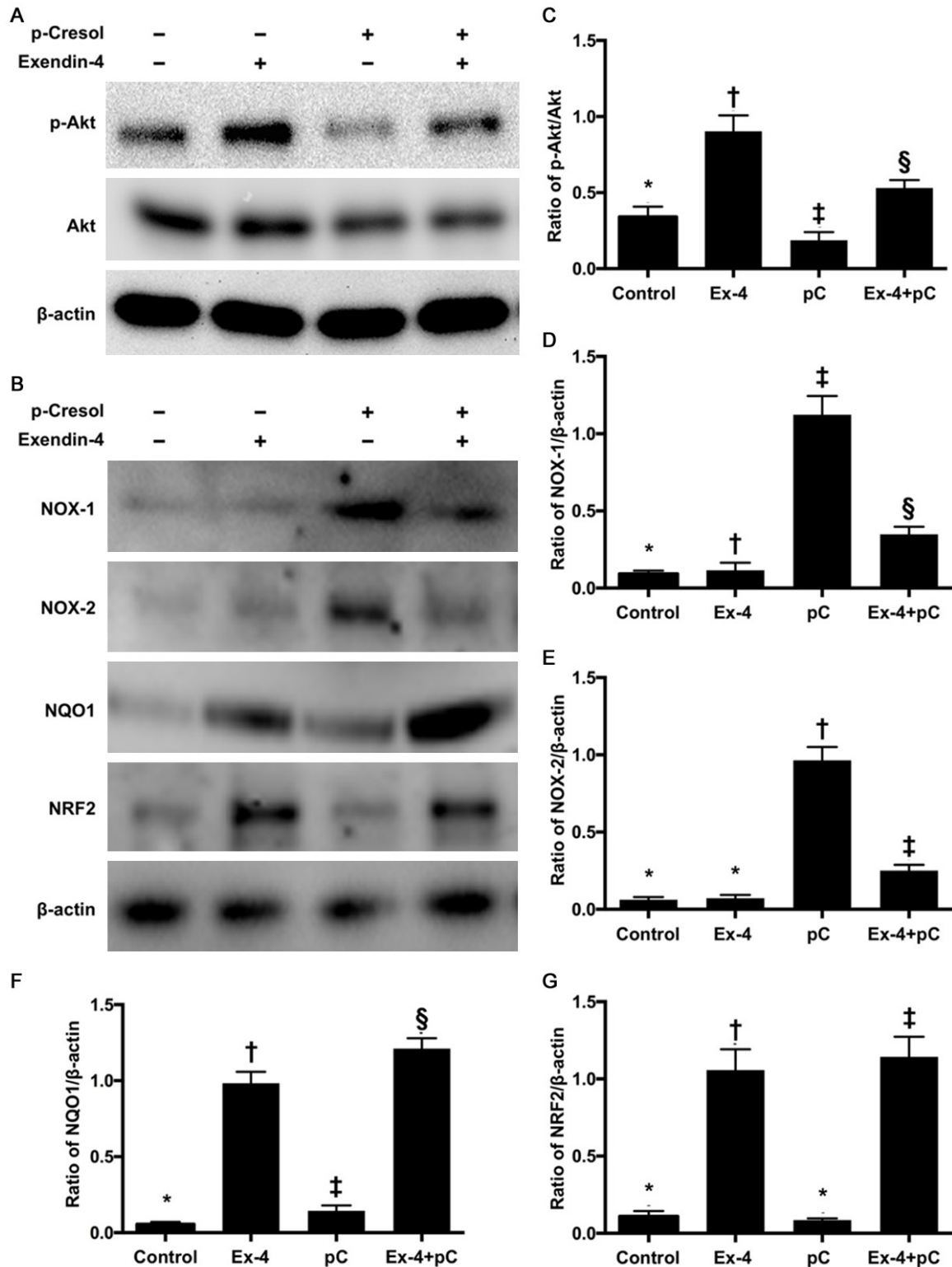


Figure 4. Competitive effects of p-cresol vs. Ex4 on protein expressions of antioxidants and oxidative stress in NRK-52E cells undergoing 24 h cell culture. A. Illustrating the protein expressions of Akt and p-Akt in the present and absent conditions of p-cresol (200 μ M) and extendin Ex4 (20 nM) treatment. B. Analytical result of ratio of p-Akt/Akt protein expression, * vs. other groups with different symbols (\dagger , \ddagger , \S), $p < 0.001$. C. Illustrating the protein expressions of NOX-1, NOX-2, NQO1 and Nrf2 in the present and absent conditions of p-cresol (200 μ M) and extendin Ex4 (20 nM) treatment. D. Analytical result of protein expression of NOX-1, * vs. other groups with different symbols (\dagger , \ddagger), $p < 0.0001$. E. Analytical result of protein expression of NOX-2, * vs. other groups with different symbols (\dagger , \ddagger), $p < 0.0001$. F. Analytical result of protein expression of NAD(P)H quinone dehydrogenase 1 (NQO1), * vs. other

Extendin-4 against IR renal injury through NRF2 signaling

groups with different symbols (†, ‡, §), $p < 0.0001$. G. Analytical result of protein expression of Nrf2, * vs. other groups with different symbols (†, ‡), $p < 0.0001$. All statistical analyses were performed by one-way ANOVA, followed by Bonferroni multiple comparison post hoc test ($n=6$ for each group). Symbols (*, †, ‡, §) indicate significance at the 0.05 level.

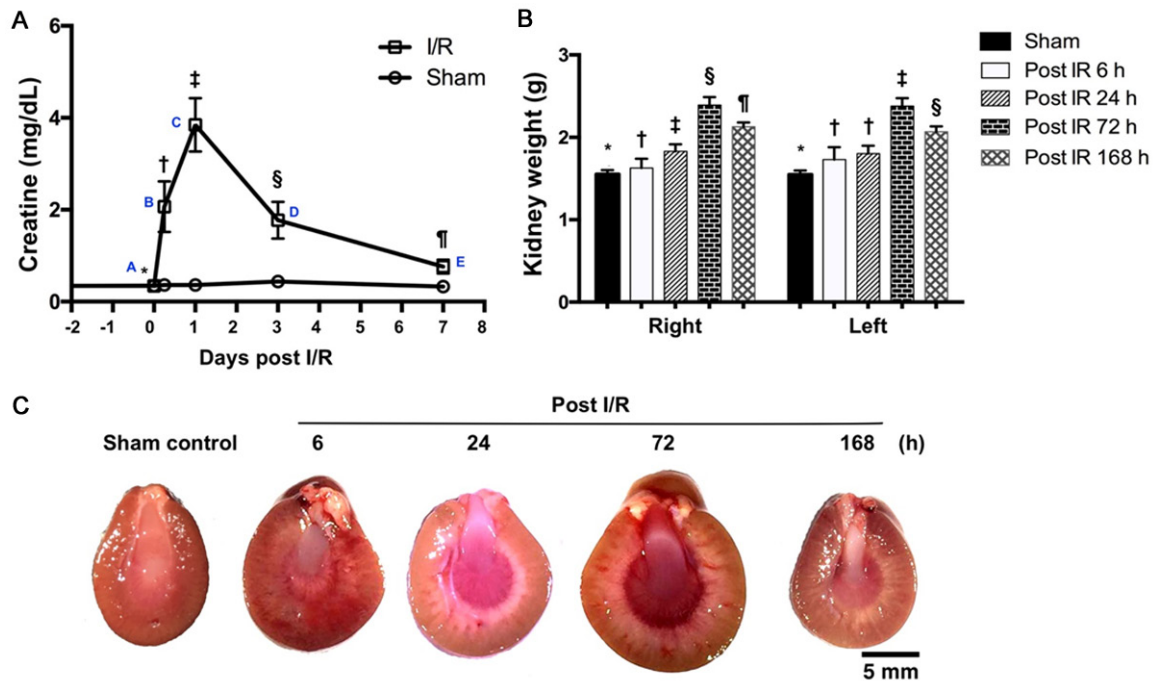


Figure 5. Time courses of circulating level of creatinine, grossly anatomical structure and rat kidney weight after IR procedure. A. Serial changes of circulating level of creatinine in rats after acute kidney injury. Analytical result, * (sham control) vs. time points (A, B, C, D) of creatinine level in acute IR group with different symbols (†, ‡, §, ¶), $p < 0.0001$. B. Analytical result of left and kidney weight in sham control and IR group. (1) Right kidney weight, * vs. other different symbols (†, ‡, §, ¶), $p < 0.0001$; (2) Left kidney weight, * vs. other different symbols (†, ‡, §, ¶), $p < 0.0001$. C. Illustrating the grossly anatomical structure in different time points after acute IR injury. The observational finding showed that the kidney size in was comparable with the kidney weight in different time intervals (i.e., 6, 72 and 168 h) after acute IR injury. All statistical analyses were performed by one-way ANOVA, followed by Bonferroni multiple comparison post hoc test ($n=6$ for each group). Symbols (*, †, ‡, §) indicate significance at the 0.05 level. IR = ischemia-reperfusion.

these two parameters were significantly reversed by Ex4 treatment (20 nM) (i.e., NRK-52E cells co-cultured with P-cresol + Ex4). On the other hand, Ex4 treatment not only augmented the protein expressions of NAD(P)H quinone dehydrogenase (NQO)-1 (i.e., an index of antioxidant), Nrf2 and p-Akt but also reversed the suppressive effect of P-cresol on these three parameters.

Time courses of circulating level of creatinine, gross anatomical structure and left/right kidney weight in Sprague Dawley (SD) rats after IR procedure (Figure 5)

The circulating level of creatinine was rapidly and significantly increased after the IR procedure. This parameter was found to be at peak level at about 24 h after the IR procedure, and

significantly and progressively decreased afterwards (i.e., decreased from days 2 to 7). Additionally, both left and right kidneys were significantly progressively increased from 6 to 24 h and up to maximal level at 72 h, then significantly decreased at the end of study period (i.e., by day 7 after the IR procedure). Interestingly, the gross anatomical structure showed that both the left and right kidney sizes were consistent with the alternation of the kidney weight at these time points.

Serial changes of monocyte chemoattractant protein-1 (MCP-1) expression under immunohistochemical (IHC) microscopic findings in kidney specimens (Figure 6)

To clarify the time courses of MCP-1 expression in kidney parenchyma, specimens were perfor-

Extendin-4 against IR renal injury through NRF2 signaling

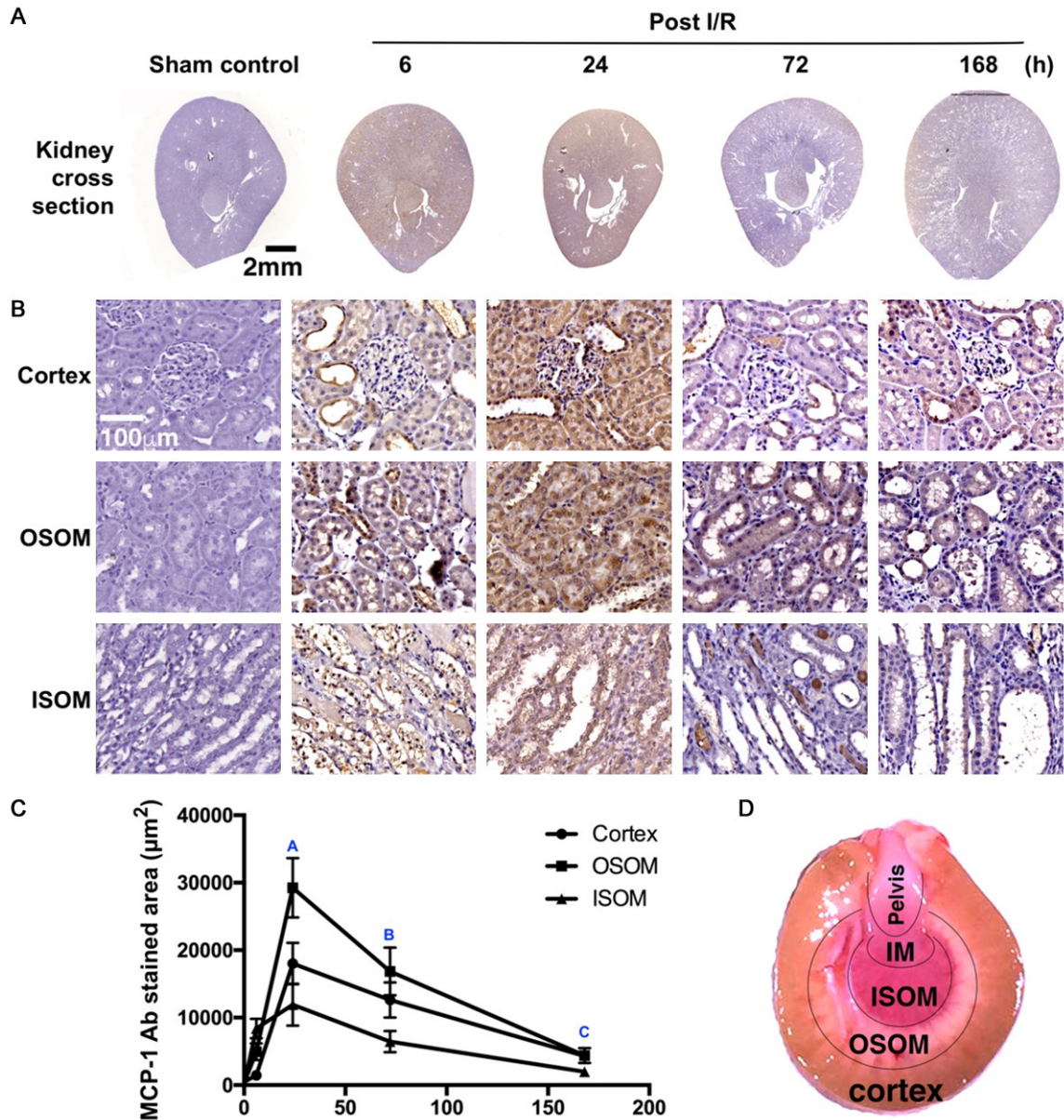


Figure 6. Serial changes of MCP-1 expressions under IHC microscopic findings in kidney specimens. A. Illustrating the time intervals (i.e., 0, 6, 24 and 168 h) of cross section of IR kidney. B. Illustrating the immunohistochemical (IHC) stain (100x) for identification of monocyte chemoattractant protein (MCP)-1 expressions (gray color) in three different anatomical layers, including (1) inner stripe of outer medulla (ISOM), (2) outer stripe of outer medulla (OSOM) and (3) cortex in different time intervals (i.e., 0, 6, 24, 72 and 168 h) after acute kidney IR procedure. C. Analytical results of MCP-1 positively stained area in rat after acute kidney IR procedure: 1) ISOM layer, baseline vs. different time points (i.e., A, B, C), $p < 0.0001$; 2) OSOM layer, baseline vs. different time points (i.e., A, B, C), $p < 0.0001$; 3) renal cortex layer, baseline vs. different time points (i.e., A, B, C), $p < 0.0001$. D. Illustrating the gross anatomical structure of kidney cross section. All statistical analyses were performed by one-way ANOVA, followed by Bonferroni multiple comparison post hoc test ($n=6$ for each group).

med at time points of baseline and 6, 24, 72 and 168 h after the IR procedure. The MCP-1 expression was analyzed in three different anatomical layers, including (1) inner stripe of outer medulla (ISOM), (2) the outer stripe of outer medulla (OSOM) and (3) the cortex. The results of IHC microscopic findings showed that the

MCP-1 positively stained area was significantly increased up to the peak level at 24 h (i.e., at the early phase of acute IR procedure) in these three layers, followed by rapidly and significantly decreasing afterwards. Additionally, this parameter was significantly higher in OSOM than in the cortex and ISOM, and significantly higher in

Extendin-4 against IR renal injury through NRF2 signaling

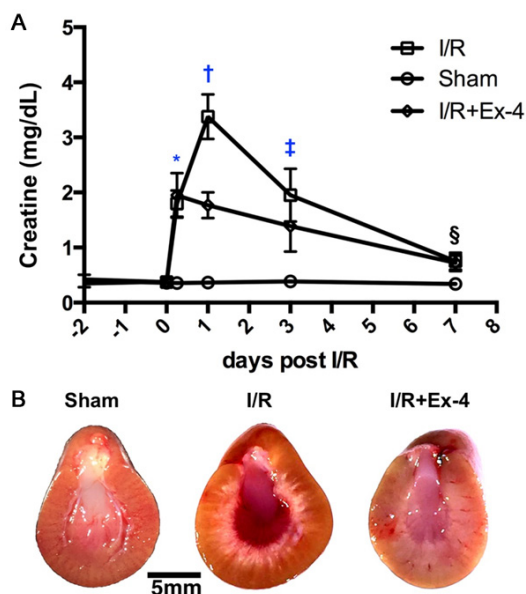


Figure 7. Time courses of circulating level of creatinine after IR procedure in three groups of animals. A. Illustrating the time courses of circulating level of creatinine at the different time intervals after acute IR procedure among the sham control, IR and IR + Ex4. (1) At baseline, sham control vs. IR and IR + Ex4, $p = 1.0$. (2) At 6 h, sham control vs. IR and IR + Ex4, $p < 0.001$. (3) At 24 h, * vs. different symbols (\dagger , \ddagger), $p < 0.0001$. Symbols (*, \dagger , \ddagger) indicate significance at the 0.05 level. (4) At 72 h, * vs. different symbols (\S , \P), $p < 0.001$. Symbols (*, \S , \P) indicate significance at the 0.05 level. (5) By day 7, * vs. #, $p < 0.0001$. B. Illustrating the grossly anatomical feature of the kidney at three groups by day 7 after acute IR injury. All statistical analyses were performed by one-way ANOVA, followed by Bonferroni multiple comparison post hoc test ($n=6$ for each group). IR = ischemia-reperfusion; Ex4 = extendin 4.

the cortex than in the ISOM at the time intervals of 6, 24 and 72 h.

Time courses of circulating level of creatinine after IR procedure in three groups of animals (Figure 7)

By day 0, the circulating level of creatinine did not differ among the group 1 (sham control), group 2 (IR) and group 3 (IR + Ex4). However, by day 1 after the IR procedure, this parameter in circulation was significantly higher in group 2 than in groups 1 and 3, and significantly higher in group 3 than in group 1. Additionally, by the time point of day 1, this parameter increased upon the peak level not only in group 2 but also in the group 3, but it did not change in the group 1. This parameter was significantly decreased afterwards among the animals of groups 2 and

3, but it was still significantly higher in group 2 than in group 3. By day 7 after the IR procedure, the circulating level of creatinine was lowest in groups 2 and 3, and did not differ between these two groups, but it was still significantly higher in groups 2 and 3 than in group 1.

MCP-1 expression by day 7 after IR procedure in kidney cortex and medulla (Figure 8)

The IHC microscopic findings showed that the MCP-1 positive staining was significantly higher in group 2 than in groups 1 and 3, and significantly higher in group 3 than in group 1 not only in the ISOM and OSOM layers but also in the renal cortex layer.

Immunofluorescence (IF) microscopic finding for identifications of Nrf2 + cells and NQO1 + cells in kidney parenchyma by day 7 after the IR procedure (Figure 9)

The IF microscopic finding showed that the number of Nrf2 + cells in the renal cortex and medullar layer were significantly higher in group 3 than in groups 1 and 2, and significantly higher in group 1 than in group 2, suggesting that upregulation of Nrf2 + cells was an intrinsic response to IR stimulation that was further upregulated by Ex4 treatment. Additionally, the number of NQO1 + cells expressed an identical pattern of Nrf2 + cells in these two layers.

Time courses of superoxide dismutase enzyme activity (U/mg) in kidney biopsy specimen after IR procedure (Figure 10)

By day 1 after IR procedure, the superoxide dismutase (SOD) activity in the kidney parenchyma was significantly higher in IR + Ex4 than in other groups, and significantly higher in the sham control (SC) + Ex4 and IR only than in SC, but it showed no difference between SC + Ex4 and IR only. By day 3 after IR procedure, this parameter was highest in IR + Ex4, lowest in IR, and significantly higher in SC + Ex4 than in SC. These results persisted until day 7 after IR procedure.

By day 1 after the IR procedure, the thickness of cortex + OSOM was significantly higher in IR and IR + Ex4 groups than in SC group, but it showed no difference between the former two groups. By days 2 and 7 after the IR procedure, this parameter was significantly higher in IR

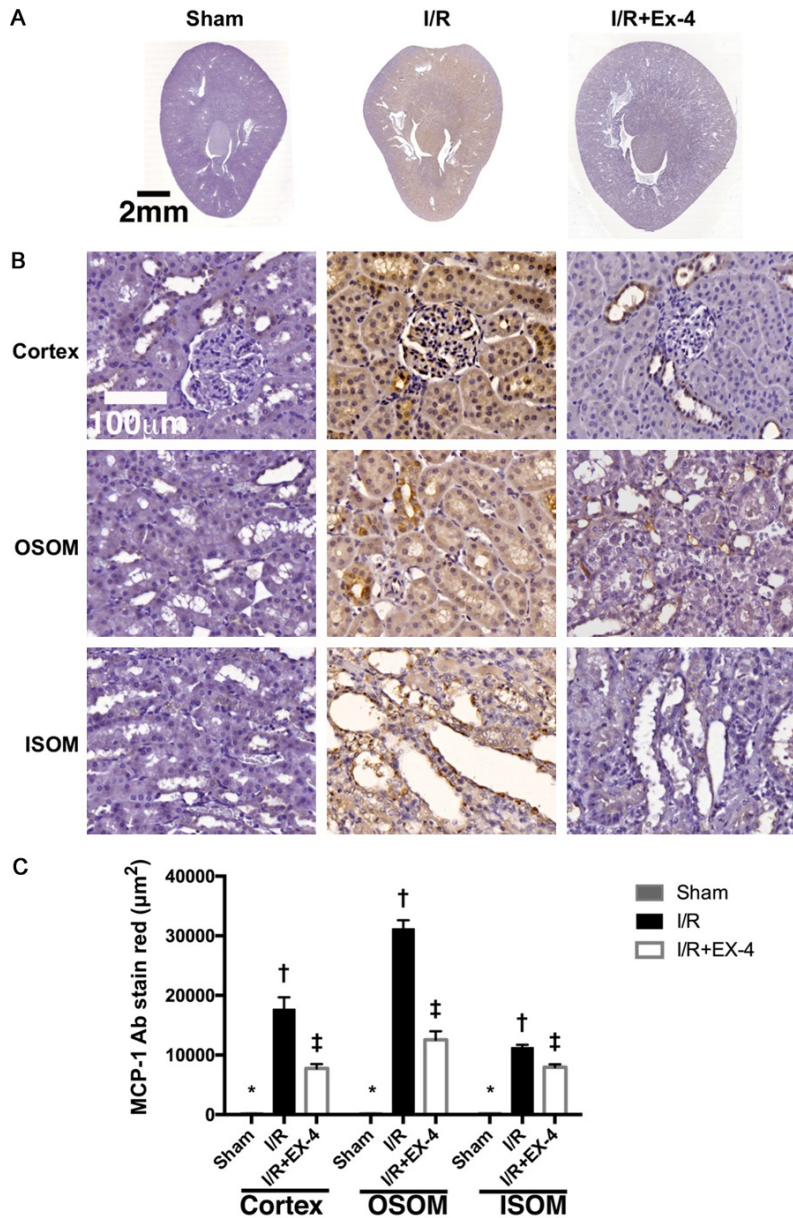


Figure 8. MCP-1 expressions by day 7 after IR procedure in kidney Cortex and Medulla. A. Showing the grossly anatomical feature of cross section of kidney among the three groups. B. Exhibiting the immunohistochemical (IHC) microscopic finding (100x) exhibited that the MCP-1 positively stained area (gray color). C. MCP-1-positively stain area in renal cortex level, * vs. other different symbols (†, ‡), $p < 0.0001$. MCP-1-positively stain area in outer stripe of outer medulla (OSOM) level, * vs. other different symbols (†, ‡), $p < 0.0001$. MCP-1-positively stain area in inner stripe of outer medulla (ISOM) level, * vs. other different symbols (†, ‡), $p < 0.0001$. All statistical analyses were performed by one-way ANOVA, followed by Bonferroni multiple comparison post hoc test ($n=6$ for each group). Symbols (*, †, ‡) indicate significance at the 0.05 level. IR = ischemia-reperfusion; Ex4 = extendin 4; MCP-1 = monocyte chemoattractant protein 1.

and IR + Ex4 groups than in SC group, and significantly higher in IR group than in IR + Ex4 groups.

Discussion

This preclinical study, conducted both in vitro and through experimental study, investigated the impact of Ex4 on protecting rat kidney from acute IR injury. The findings have several implications. First, P-cresol, a uremic toxic compound, was identified to significantly upregulate oxidative stress (i.e., NOX-1, NOX-2) and downregulate an antioxidant (i.e., Nrf2) and the cell survival and growth signaling (i.e., Akt/PKB) in cultured NRK-52E cells (i.e., a rat renal proximal tubular cells). On the other hand, Ex4 reversed the effect of P-cresol through enhancing the production of antioxidants (i.e., Nrf2, NQO1). Second, an experimental model of acute kidney IR was successfully created. An important finding was that the time courses of creatinine level, kidney weight and inflammatory response were precisely identified in the acute kidney IR setting. Third, the protective effects of Ex4 on kidney function and architecture were found to be mainly through augmenting the generation of antioxidants and suppressing the expression of oxidative stress and inflammation.

Previous studies have clearly shown that p-Cresol, one of the most important uremic toxins, increases oxidative stress and inactivates Akt activity in cells and rodents [34-36]. One important finding in our in vitro study was that the protein expression of anti-oxidants and cell survival signaling were remarkably downregulated and the protein

Extentin-4 against IR renal injury through NRF2 signaling

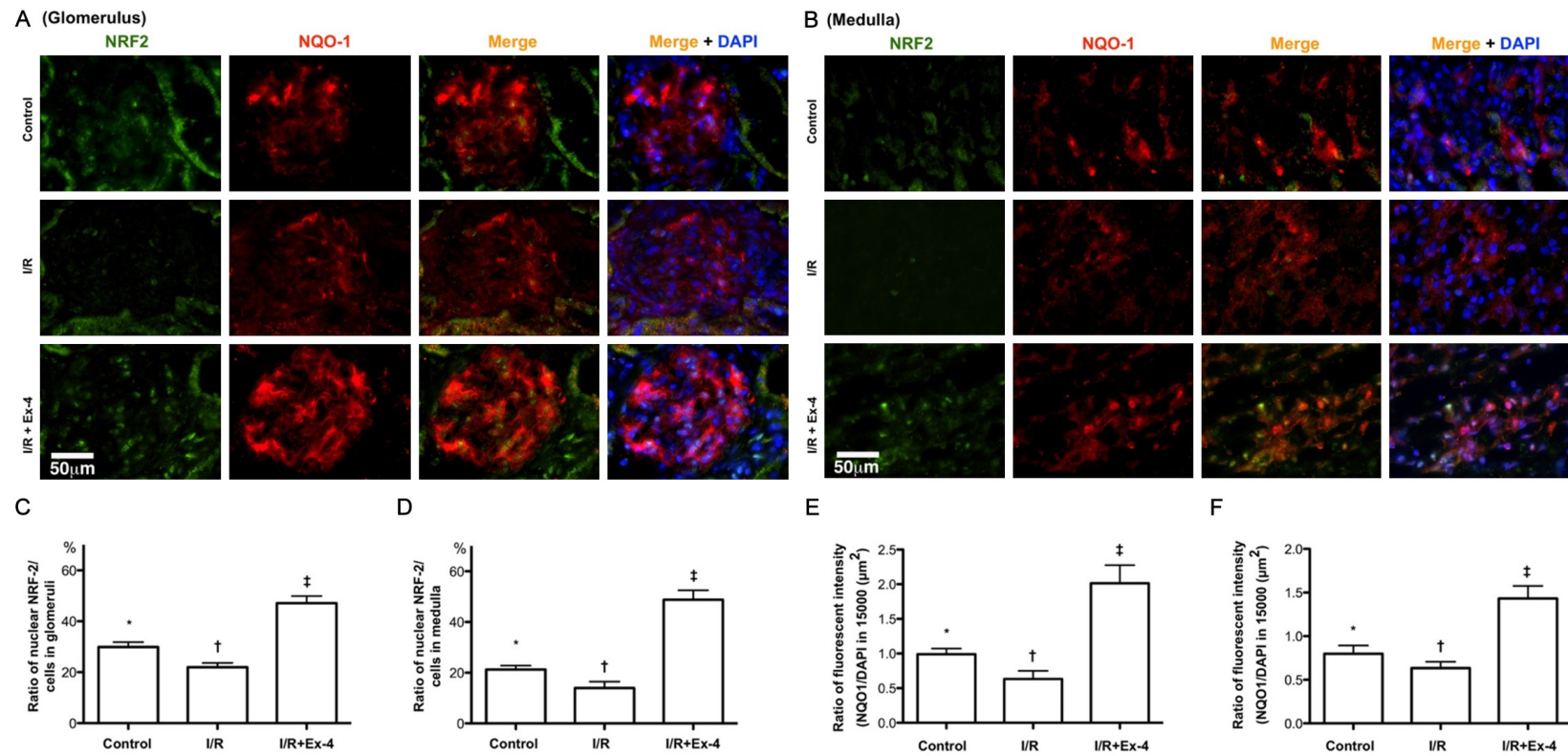


Figure 9. Cellular expressions of Nrf2 + cells and NQO1 + cells in kidney parenchyma by day 7 after IR procedure. A. Illustrating the IF microscopic finding (200x) for identification of Nrf2 + cells (green color) and NQO1 + cells (red color) in glomeruli among the three groups. B. Illustrating the IF microscopic finding (200x) for identification of Nrf2 + cells (green color) and NQO1 + cells (red color) in medulla among the three groups. C. Analytic results of number of Nrf2 + cells in glomeruli, * vs. other groups with different symbols (†, ‡), $p < 0.001$. D. Analytic results of number of NQO1 + cells in glomeruli, * vs. other groups with different symbols (†, ‡), $p < 0.001$. E. Analytic results of number of Nrf2 + cells in glomeruli, * vs. other groups with different symbols (†, ‡), $p < 0.001$. F. Analytic results of number of NQO1 + cells in medulla, * vs. other groups with different symbols (†, ‡), $p < 0.001$. All statistical analyses were performed by one-way ANOVA, followed by Bonferroni multiple comparison post hoc test ($n=6$ for each group). Symbols (*, †, ‡) indicate significance at the 0.05 level. IR = ischemia-reperfusion; Ex4 = exentin 4.

Exendin-4 against IR renal injury through NRF2 signaling

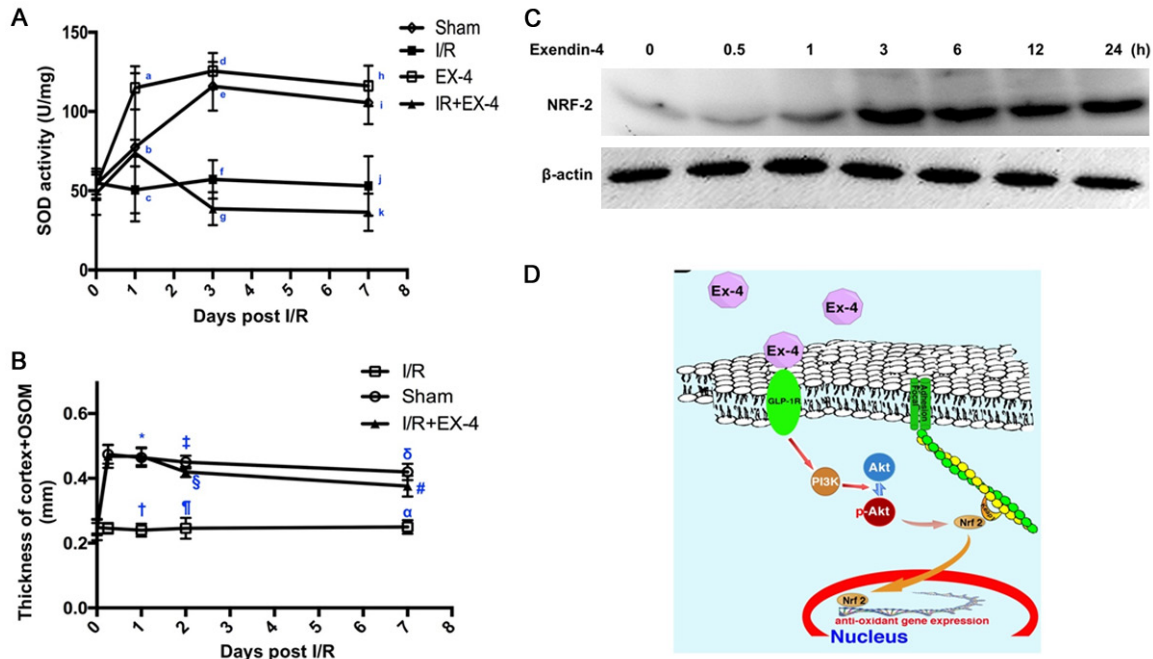


Figure 10. Time courses of superoxide dismutase (SOD) enzyme activity (U/mg) in kidney parenchyma and thickness of renal cortex + outer stripe of outer medulla (OSOM) after IR procedure. **A.** Time courses of SOD activity in kidney parenchyma among three groups of animals. Analytical results: (1) By day 1, a vs. different letters (b, c) in different groups, $p < 0.0001$, letters (a, b, c) indicate significance at the 0.05 level; (2) By day 3, d vs. different letters (e, f, g) in different groups, $p < 0.0001$, letters (d, e, f, g) indicate significance at the 0.05 level; (3) By day 7, h vs. different letters (i, j, k) in different groups, $p < 0.0001$, letters (h, i, j, k) indicate significance at the 0.05 level. **B.** Time courses of thickness of cortex + OSOM. Analytical results: (1) by day 1, * vs. †, $p < 0.0001$; (2) by day 2, ‡ vs. different groups with different symbols (§, ¶), $p < 0.0001$, symbols (*, †, ‡) indicate significance at the 0.05 level; (3) by day 7, δ vs. different groups with different symbols (#, α), $p < 0.0001$, symbols (#, α, δ) indicate significance at the 0.05 level. All statistical analyses were performed by one-way ANOVA, followed by Bonferroni multiple comparison post hoc test ($n = 6$ for each group). IR = ischemia-reperfusion; Ex4 = exendin 4. **C.** Illustrating the time courses of protein expressions of Nrf2 undergoing exendin-4 (20 nM) stimulation. **D.** Proposed mechanisms underlying the positive therapeutic effects of exendin-4 on enhancing the generation of antioxidants for protecting the kidney from acute ischemia-reperfusion (IR) injury. Ex-4 = exendin 4; GLP-1R = glucagon-like peptide 1 receptor.

expression of oxidative stress and inflammation were markedly upregulated in NRK-52E cells co-cultured with P-cresol compound. Our findings were consistent with the findings of previous studies [34-36]. Of importance, these parameters (i.e., oxidative stress/anti-oxidants/cell-survival signaling) were notably revised after Ex4 treatment. Intriguingly, Nrf2 activated the expressions of antioxidants and phase 2 enzymes to protect the cells/organs against oxidative stress-induced damage [37-40]. GLP-1/GLP-1R signaling regulates the enzymatic system of anti-oxidation in acute kidney injury, diabetic nephropathy, and other renal damage [28, 33, 41-44]. The results of our in vitro studies in addition to being consistent with the findings of previous studies [28, 33, 37-44], explained that Ex4 had a cellular (NRK-52E cells) protective effect mainly through down-regulation of oxidative stress and upregulation of antioxidants.

Rapidly increasing circulating creatinine has been well recognized in our previous experimental studies [28, 45-47]. Interestingly, the time courses of circulating level of creatinine have been infrequently assessed. A principal finding in the present study was that not only the time courses of the circulating level was accurately measured but also the peak level of circulating creatinine was clearly identified. In addition, the serial changes of left and right kidney weight and also an increase in peak value of kidney weight (i.e., an indicator of kidney swelling/edema with fluid accumulation) was established in rats after acute kidney IR injury. These preclinical findings may provide important clinical information for our daily clinical practice in management of those patients with AKI along with the most suitable time for pharmacological intervention.

There is an association between acute kidney IR injury and enhancement of the inflammatory

reaction which in turn further damages the kidney function and anatomical structure [28, 32, 33, 45-47]. Additionally, some studies have further demonstrated that Ex4 therapy significantly suppressed the inflammatory reaction and upregulation of anti-oxidants at the molecular and cellular levels [28, 32, 33, 45-47]. An essential finding of the present study was that the IHC microscopic finding demonstrated that as compared with SC, the expression of MCP-1 (i.e., an indicator of inflammation) in IR animals was significantly increased kidney parenchyma, including in the renal cortex and medulla. Our finding was consistent with the findings of previous studies [28, 32, 33, 45-47]. The most important finding in the present study was that Ex4 therapy significantly suppressed the expression of MCP-1 and upregulations of NQO1, Nrf2 and SOD in rat kidney after the acute IR procedure. In this way, our findings in addition to reinforcing the findings of previous studies, explained why the thickness of the renal cortex-OSOM (an indicator of damaged the integrity of kidney architecture) was remarkably reduced in IR + Ex4 animals in comparison to in those of IR-only animals.

Study limitations

This study has limitations. First, the study period was only 7 days; therefore, the long-term effect of Ex4 therapy on protecting the kidney remains uncertain. Second, although plentiful data support the effect of Ex4 therapy on protecting the renal function and kidney architecture, the exact underlying mechanisms of this therapy is still not completely clear in the present study. The proposed mechanisms underlying the observed protection of Ex4 treatment against acute kidney IR injury based on our findings have been summarized in **Figure 10C**.

In conclusion, Ex4 therapy protected kidney architecture and function through Akt/PKB-Nrf2-independent signaling to upregulate anti-oxidants to counteract the oxidative-stress effect.

Acknowledgements

This study was supported by a program grant from Chang Gung Memorial Hospital, Chang Gung University (Grant number: CMRPG8E13-31).

Disclosure of conflict of interest

None.

Address correspondence to: Dr. Sheung-Fat Ko, Department of Radiology, Kaohsiung Chang Gung Memorial Hospital and Chang Gung University College of Medicine, No. 123, Da-Pei Rd., Niao-Sung District, Kaohsiung 83301, Taiwan. Tel: +886 7 7317123 ext. 2579; Fax: +886-7-7318362; E-mail: kosheung-fat@gmail.com; Dr. Hon-Kan Yip, Division of Cardiology, Kaohsiung Chang Gung Memorial Hospital and Chang Gung University College of Medicine, No. 123, Da-Pei Rd., Niao-Sung District, Kaohsiung 83301, Taiwan. Tel: +886 7 7317123 ext. 8300; Fax: +886 7 7322402; E-mail: han.gung@msa.hinet.net

References

- [1] Duranton F, Cohen G, De Smet R, Rodriguez M, Jankowski J, Vanholder R, Argiles A; European Uremic Toxin Work Group. Normal and pathologic concentrations of uremic toxins. *J Am Soc Nephrol* 2012; 23: 1258-1270.
- [2] Masereeuw R, Mutsaers HA, Toyohara T, Abe T, Jhavar S, Sweet DH and Lowenstein J. The kidney and uremic toxin removal: glomerulus or tubule? *Semin Nephrol* 2014; 34: 191-208.
- [3] Lekawanvijit S, Kompa AR, Wang BH, Kelly DJ and Krum H. Cardiorenal syndrome: the emerging role of protein-bound uremic toxins. *Circ Res* 2012; 111: 1470-1483.
- [4] Parikh CR, Coca SG, Wang Y, Masoudi FA and Krumholz HM. Long-term prognosis of acute kidney injury after acute myocardial infarction. *Arch Intern Med* 2008; 168: 987-995.
- [5] Friedericksen DV, Van der Merwe L, Hattingh TL, Nel DG and Moosa MR. Acute renal failure in the medical ICU still predictive of high mortality. *S Afr Med J* 2009; 99: 873-875.
- [6] Lameire N, Van Biesen W and Vanholder R. Acute renal failure. *Lancet* 2005; 365: 417-430.
- [7] Sementilli A and Franco M. Renal acute cellular rejection: correlation between the immunophenotype and cytokine expression of the inflammatory cells in acute glomerulitis, arterial intimitis, and tubulointerstitial nephritis. *Transplant Proc* 2010; 42: 1671-1676.
- [8] Chen YT, Sun CK, Lin YC, Chang LT, Chen YL, Tsai TH, Chung SY, Chua S, Kao YH, Yen CH, Shao PL, Chang KC, Leu S and Yip HK. Adipose-derived mesenchymal stem cell protects kidneys against ischemia-reperfusion injury through suppressing oxidative stress and inflammatory reaction. *J Transl Med* 2011; 9: 51.
- [9] Sun CK, Yen CH, Lin YC, Tsai TH, Chang LT, Kao YH, Chua S, Fu M, Ko SF, Leu S and Yip HK. Autologous transplantation of adipose-derived mesenchymal stem cells markedly reduced acute ischemia-reperfusion lung injury in a rodent model. *J Transl Med* 2011; 9: 118.

Exendin-4 against IR renal injury through NRF2 signaling

- [10] Chertow GM, Burdick E, Honour M, Bonventre JV and Bates DW. Acute kidney injury, mortality, length of stay, and costs in hospitalized patients. *J Am Soc Nephrol* 2005; 16: 3365-3370.
- [11] Srisawat N and Kellum JA. Acute kidney injury: definition, epidemiology, and outcome. *Curr Opin Crit Care* 2011; 17: 548-555.
- [12] Vanholder R, Glorieux G, De Smet R, Lameire N; European Uremic Toxin Work Group. New insights in uremic toxins. *Kidney Int Suppl* 2003; S6-10.
- [13] Satoh M, Hayashi H, Watanabe M, Ueda K, Yamato H, Yoshioka T and Motojima M. Uremic toxins overload accelerates renal damage in a rat model of chronic renal failure. *Nephron Exp Nephrol* 2003; 95: e111-118.
- [14] Pickering JW, James MT and Palmer SC. Acute kidney injury and prognosis after cardiopulmonary bypass: a meta-analysis of cohort studies. *Am J Kidney Dis* 2015; 65: 283-293.
- [15] Coca SG, Yusuf B, Shlipak MG, Garg AX and Parikh CR. Long-term risk of mortality and other adverse outcomes after acute kidney injury: a systematic review and meta-analysis. *Am J Kidney Dis* 2009; 53: 961-973.
- [16] de Mendonca A, Vincent JL, Suter PM, Moreno R, Dearden NM, Antonelli M, Takala J, Sprung C and Cantraine F. Acute renal failure in the ICU: risk factors and outcome evaluated by the SOFA score. *Intensive Care Med* 2000; 26: 915-921.
- [17] Groeneveld AB, Tran DD, van der Meulen J, Nauta JJ and Thijs LG. Acute renal failure in the medical intensive care unit: predisposing, complicating factors and outcome. *Nephron* 1991; 59: 602-610.
- [18] Liotta M, Olsson D, Sartipy U and Holzmann MJ. Minimal changes in postoperative creatinine values and early and late mortality and cardiovascular events after coronary artery bypass grafting. *Am J Cardiol* 2014; 113: 70-75.
- [19] Hobson CE, Yavas S, Segal MS, Schold JD, Tribble CG, Layon AJ and Bihorac A. Acute kidney injury is associated with increased long-term mortality after cardiothoracic surgery. *Circulation* 2009; 119: 2444-2453.
- [20] Bihorac A, Yavas S, Subbiah S, Hobson CE, Schold JD, Gabrielli A, Layon AJ and Segal MS. Long-term risk of mortality and acute kidney injury during hospitalization after major surgery. *Ann Surg* 2009; 249: 851-858.
- [21] Lafrance JP and Miller DR. Acute kidney injury associates with increased long-term mortality. *J Am Soc Nephrol* 2010; 21: 345-352.
- [22] Li B, Cohen A, Hudson TE, Motlagh D, Amrani DL and Duffield JS. Mobilized human hematopoietic stem/progenitor cells promote kidney repair after ischemia/reperfusion injury. *Circulation* 2010; 121: 2211-2220.
- [23] Chen HH, Lin KC, Wallace CG, Chen YT, Yang CC, Leu S, Chen YC, Sun CK, Tsai TH, Chen YL, Chung SY, Chang CL and Yip HK. Additional benefit of combined therapy with melatonin and apoptotic adipose-derived mesenchymal stem cell against sepsis-induced kidney injury. *J Pineal Res* 2014; 57: 16-32.
- [24] Chen Q, Camara AK, Stowe DF, Hoppel CL and Lesnefsky EJ. Modulation of electron transport protects cardiac mitochondria and decreases myocardial injury during ischemia and reperfusion. *Am J Physiol Cell Physiol* 2007; 292: C137-147.
- [25] Chen Q, Moghaddas S, Hoppel CL and Lesnefsky EJ. Ischemic defects in the electron transport chain increase the production of reactive oxygen species from isolated rat heart mitochondria. *Am J Physiol Cell Physiol* 2008; 294: C460-466.
- [26] Hirayama A, Nagase S, Ueda A, Oteki T, Takada K, Obara M, Inoue M, Yoh K, Hirayama K and Koyama A. In vivo imaging of oxidative stress in ischemia-reperfusion renal injury using electron paramagnetic resonance. *Am J Physiol Renal Physiol* 2005; 288: F597-603.
- [27] Nilakantan V, Hilton G, Maenpaa C, Van Why SK, Pieper GM, Johnson CP and Shames BD. Favorable balance of anti-oxidant/pro-oxidant systems and ablated oxidative stress in Brown Norway rats in renal ischemia-reperfusion injury. *Mol Cell Biochem* 2007; 304: 1-11.
- [28] Chen YT, Tsai TH, Yang CC, Sun CK, Chang LT, Chen HH, Chang CL, Sung PH, Zhen YY, Leu S, Chang HW, Chen YL and Yip HK. Exendin-4 and sitagliptin protect kidney from ischemia-reperfusion injury through suppressing oxidative stress and inflammatory reaction. *J Transl Med* 2013; 11: 270.
- [29] Sheu JJ, Chang MW, Wallace CG, Chiang HJ, Sung PH, Tsai TH, Chung SY, Chen YL, Chua S, Chang HW, Sun CK, Lee FY and Yip HK. Exendin-4 protected against critical limb ischemia in obese mice. *Am J Transl Res* 2015; 7: 445-459.
- [30] Oeseburg H, de Boer RA, Buikema H, van der Harst P, van Gilst WH and Sillje HH. Glucagon-like peptide 1 prevents reactive oxygen species-induced endothelial cell senescence through the activation of protein kinase A. *Arterioscler Thromb Vasc Biol* 2010; 30: 1407-1414.
- [31] Chua S, Lee FY, Chiang HJ, Chen KH, Lu HI, Chen YT, Yang CC, Lin KC, Chen YL, Kao GS, Chen CH, Chang HW and Yip HK. The cardioprotective effect of melatonin and exendin-4 treatment in a rat model of cardiorenal syndrome. *J Pineal Res* 2016; 61: 438-456.
- [32] Chen KH, Chen CH, Wallace CG, Chen YT, Yang CC, Sung PH, Chiang HJ, Chen YL, Chua S, Yip

Exendin-4 against IR renal injury through NRF2 signaling

- HK and Cheng JT. Combined therapy with melatonin and exendin-4 effectively attenuated the deterioration of renal function in rat cardio-renal syndrome. *Am J Transl Res* 2017; 9: 214-229.
- [33] Yip HK, Yang CC, Chen KH, Huang TH, Chen YL, Zhen YY, Sung PH, Chiang HJ, Sheu JJ, Chang CL, Chen CH, Chang HW and Chen YT. Combined melatonin and exendin-4 therapy preserves renal ultrastructural integrity after ischemia-reperfusion injury in the male rat. *J Pineal Res* 2015; 59: 434-447.
- [34] Noh H, Yu MR, Kim HJ, Jang EJ, Hwang ES, Jeon JS, Kwon SH and Han DC. Uremic toxin p-cresol induces Akt-pathway-selective insulin resistance in bone marrow-derived mesenchymal stem cells. *Stem Cells* 2014; 32: 2443-2453.
- [35] Chang MC, Chang HH, Chan CP, Yeung SY, Hsien HC, Lin BR, Yeh CY, Tseng WY, Tseng SK and Jeng JH. p-Cresol affects reactive oxygen species generation, cell cycle arrest, cytotoxicity and inflammation/atherosclerosis-related modulators production in endothelial cells and mononuclear cells. *PLoS One* 2014; 9: e114446.
- [36] Koppe L, Pillon NJ, Vella RE, Croze ML, Pelletier CC, Chambert S, Massy Z, Glorieux G, Vanholder R, Dugenet Y, Soula HA, Fouque D and Soulage CO. p-Cresyl sulfate promotes insulin resistance associated with CKD. *J Am Soc Nephrol* 2013; 24: 88-99.
- [37] Zhang M, An C, Gao Y, Leak RK, Chen J and Zhang F. Emerging roles of Nrf2 and phase II antioxidant enzymes in neuroprotection. *Prog Neurobiol* 2013; 100: 30-47.
- [38] Zhu H, Itoh K, Yamamoto M, Zweier JL and Li Y. Role of Nrf2 signaling in regulation of antioxidants and phase 2 enzymes in cardiac fibroblasts: protection against reactive oxygen and nitrogen species-induced cell injury. *FEBS Lett* 2005; 579: 3029-3036.
- [39] Li KR, Yang SQ, Gong YQ, Yang H, Li XM, Zhao YX, Yao J, Jiang Q and Cao C. 3H-1,2-dithiole-3-thione protects retinal pigment epithelium cells against Ultra-violet radiation via activation of Akt-mTORC1-dependent Nrf2-HO-1 signaling. *Sci Rep* 2016; 6: 25525.
- [40] Li W, Khor TO, Xu C, Shen G, Jeong WS, Yu S and Kong AN. Activation of Nrf2-antioxidant signaling attenuates NF-kappaB-inflammatory response and elicits apoptosis. *Biochem Pharmacol* 2008; 76: 1485-1489.
- [41] Fujita H, Morii T, Fujishima H, Sato T, Shimizu T, Hosoba M, Tsukiyama K, Narita T, Takahashi T, Drucker DJ, Seino Y and Yamada Y. The protective roles of GLP-1R signaling in diabetic nephropathy: possible mechanism and therapeutic potential. *Kidney Int* 2014; 85: 579-589.
- [42] Glastras SJ, Chen H, McGrath RT, Zaky AA, Gill AJ, Pollock CA and Saad S. Effect of GLP-1 Receptor Activation on Offspring Kidney Health in a Rat Model of Maternal Obesity. *Sci Rep* 2016; 6: 23525.
- [43] Kahal H, Abouda G, Rigby AS, Coody AM, Kilpatrick ES and Atkin SL. Glucagon-like peptide-1 analogue, liraglutide, improves liver fibrosis markers in obese women with polycystic ovary syndrome and nonalcoholic fatty liver disease. *Clin Endocrinol (Oxf)* 2014; 81: 523-528.
- [44] Filippatos TD and Elisaf MS. Effects of glucagon-like peptide-1 receptor agonists on renal function. *World J Diabetes* 2013; 4: 190-201.
- [45] Chen YT, Yang CC, Zhen YY, Wallace CG, Yang JL, Sun CK, Tsai TH, Sheu JJ, Chua S, Chang CL, Cho CL, Leu S and Yip HK. Cyclosporine-assisted adipose-derived mesenchymal stem cell therapy to mitigate acute kidney ischemia-reperfusion injury. *Stem Cell Res Ther* 2013; 4: 62.
- [46] Chang YC, Hsu SY, Yang CC, Sung PH, Chen YL, Huang TH, Kao GS, Chen SY, Chen KH, Chiang HJ, Yip HK and Lee FY. Enhanced protection against renal ischemia-reperfusion injury with combined melatonin and exendin-4 in a rodent model. *Exp Biol Med (Maywood)* 2016; 241: 1588-1602.
- [47] Lin KC, Yip HK, Shao PL, Wu SC, Chen KH, Chen YT, Yang CC, Sun CK, Kao GS, Chen SY, Chai HT, Chang CL, Chen CH and Lee MS. Combination of adipose-derived mesenchymal stem cells (ADMSC) and ADMSC-derived exosomes for protecting kidney from acute ischemia-reperfusion injury. *Int J Cardiol* 2016; 216: 173-185.